IEEE Access
Multidisciplinary ⋮ Rapid Review ⋮ Open Access Journal

Received April 30, 2020, accepted May 15, 2020, date of publication May 27, 2020, date of current version June 11, 2020.

Digital Object Identifier 10.1109/ACCESS.2020.2997919

Numerical Study on the Influence of Altitude on Roof Temperature in Mine Fires

E WU[1], RUI HUANG[1], LIN WU[1,2], XUE SHEN[1], AND ZEYOU LI[1]

[1]School of Resources and Safety Engineering, Central South University, Changsha 410083, China
[2]Safety & Security Theory Innovation and Promotion Center (STIPC), Central South University, Changsha 410083, China

Corresponding author: Rui Huang (huangrui@csu.edu.cn)

This work was supported by the National Key Research and Development Program of China (No. 2018YFC0808406) and the Research on the Scenario Construction and Emergency Management System in High-altitude Mine Fire (No. 2020zzts703).

ABSTRACT The temperature distribution of the roadway roof in a mine fire is closely related to the internal environment of the mine, which changes by the mine's altitude. In order to accurately reveal the distribution of roof temperature in mine fires at different elevations, altitude should be considered as avariable. Using FDS (Fire Dynamic Simulator), six fire sources of different scales are designed to simulate fire scenarios at five different altitudes from 0 to 4,000 m (equal diversion point). The roof temperature distribution along the longitudinal centerline of the tunnel is obtained. At the same time, the influence of high temperature on the roof support of the roadway is analyzed when the mine's altitude changes. The results show that when the fire heat release rate is relatively small, the combustion belongs to fuel-controlled combustion, and the roof temperature rises with altitude. As the heat release rate continues to increase, the roof temperature decreases with increasing altitude, which is mainly due to the low-oxygen environment in plateau areas. In addition, mine fires at normal altitudes (altitude $<$ 3,000 m) are less affected by altitude changes, and the roof temperature is always positively related to fire heat release rate. However, high altitude has an inhibitory effect on fire. In the initial stage of continuously expanding the heat release rate, There is still a positive correlation between the roof temperature and the heat release rate. When the heat release rate increases to 100 MW, the roof temperature distribution does not continue to increase. Instead, it remains stable, and the higher the altitude, the lower the stable value. Finally, based on the combination of dimensional analysis and dimensionless analysis, a correlation for predicting the longitudinal distribution of roof temperature in mine fires at different altitudes is established. The predicted data of this empirical model is highly consistent with the measured data.

INDEX TERMS Mine fire, altitude, roof temperature, temperature distribution, numerical simulation.

I. INTRODUCTION

Mineral resources are important material basis of social development and the national economy. With the continuous mineral development, people have turned their attention from the mainland to higher altitude areas. At present, a large number of mining projects in high altitude areas have been completed. In the process of mining, various calamity accidents often occur. Especially mine fires are complex, lasting and costly catastrophic accidents worldwide [1]. Because of being in the confined space, the high-temperature smoke generated by the fire is difficult to dissipate quickly, and gradually fill the whole underground space. The smoke accumulates under the roof during the spreading process and exchanges heat with the tunnel lining continuously. As a result, the stress of the roof strata changes, and the roadway support is damaged, which brings potential safety hazards to the production process of the mine [2]. For example, the change in the stress of the roof strata caused by a fire is likely to quietly breed roof accidents such as roof fall, resulting in casualties. If rescuers enter the mine without detecting the deformation of surrounding rock structures, the risk of rescue will increase greatly. Besides, a large amount of heat is generated by the burning of materials in the fire, which changes the surrounding temperature. Simultaneously, temperature detectors are usually installed in the vault to respond to temperature changes in a point or around a line in the warning range. Therefore, it is helpful to clarify the roof temperature distribution of the fire to rationally select, set, and improve the detector. However, the roof temperature in

The associate editor coordinating the review of this manuscript and approving it for publication was Giovanni Angiulli.

the mine fire is closely related to the internal environment of the mine. At the same time, environmental parameters such as atmospheric pressure, temperature and air density at different altitudes are varied, which will significantly affect the fire dynamics and smoke behavior [3]–[5]. Therefore, studying the distribution of roof temperature in mine fires at different altitudes is not only related to the prevention and control of mine fires when mine's altitudes are different, but also has important practical significance for the prevention of roof accidents and the effective use of energy.

At present, there are many research achievements on variable pressure, but they are mainly limited to the analysis of combustion characteristics of simple sources, such as burning rate [6]–[8], flame height [9], [10] and flame temperature [9]–[11] and other parameters. Some studies on the analysis of smoke movement and ceiling temperature in tunnel fires from the pressure perspective have also been reported [12], [13]. It was found that the air entrainment coefficient becomes smaller, the ceiling temperature increases, and the temperature dropped more rapidly at lower pressures. Ji *et al.* [14] simulated tunnel fires at six typical pressures, and the results showed that the temperature of longitudinal distribution increased with the decreasing pressure due to the decrease of air density and air entrainment. Besides, the dimensionless temperature rise in the longitudinal direction of the tunnel decreases exponentially against dimensionless distance. However, few studies consider altitude and pay attention to the evolution of mine fires. Yan *et al.* [15] conducted fire tests in a road tunnel at an altitude of 4,100 m to study fire heat release rate, temperature distribution, smoke propagation and back-layering, and compared the experimental results with the normal altitude of 773 m. The results showed that the decay rate of dimensionless temperature in the former case is higher than that in the latter, and the plume temperature and flame height are higher than those at 773 m above sea level. Zhang *et al.* [16] conducted large-scale and small-scale experiments in a tunnel with an altitude of 3,510 meters, and analyzed the characteristics of combustion and smoke distribution. It was found that under the conditions of pool fires of the same size, fire heat release rate (HRR) in high-altitude areas was significantly lower than that in low altitude areas, the burning time was longer, and the visibility near the fire was reduced. However, the above research either merely considers the effect of environmental pressure, or only focuses on the simple comparison of fires at the high altitude and the normal altitude. They are relatively lacking in universality, and are far from enough to truly recognize the smoke behavior and the evolution law of the roof temperature in mine fires at different altitudes.

As far as the research of mine fires is concerned, field experiments require huge investment in human, material and financial resources. At the same time, the fire experiments also have a large risk probability. Therefore, FDS (Fire Dynamic Simulator) was used to simulate the mine fire, and fire scenarios with longitudinal ventilation at five different altitudes varied from 0 to 4,000 m were simulated. Focusing on the roof temperature distribution in fires, and combining with the existing theoretical basis of mine fires at the conventional altitude, the temperature distribution of mine fires at five altitudes is compared and analyzed. It is expected to provide a reference for selecting roadway support schemes and organizing emergency rescue of mines at different altitudes.

II. CONVENTION

The temperature in a mine fire depends on many factors. However, for the research variable ''mines at different altitudes'' in the current study, it is difficult to ensure that all control variables have a one-to-one correspondence with altitude. Therefore, in order to avoid complicating the research and making the research conclusions clear, the following conventions are formulated.

(1) Different disciplines have different understandings of ''plateau'' and ''environment'', and their definitions are also different. Among them, altitude medicine and physiology define the height at which the human body experiences altitude reaction as plateau. Usually, when the human body is located more than 3,000 meters, the human organs will have an altitude reaction to varying degrees. Therefore, the subject thinks that the area with an altitude of more than 3,000 meters (including 3, 000 m) is the plateau. The high-altitude mines are mines with an altitude of more than or equal to 3,000 m in the current study. Conventional or normal mines refer to mines with an altitude of less than 3000 m.

(2) Changes in altitude will directly drive changes in various environmental parameters in the atmosphere, among which the influence of environmental temperature, atmospheric pressure, air density and oxygen concentration on fire and smoke movement is relatively large. Therefore, it is assumed that these four parameters are varied under different altitude conditions. Other environmental parameters are considered to be consistent with the plain areas, and their specific values are specified by default within the Pyrosim software.

(3) The natural environment of the mine, such as ventilation, geothermal, human factors, and equipment factors, will cause the temperature in the mine tunnel to change in varying degrees. The influence of these factors on the temperature in the tunnel is ignored when the altitude of the mine changes.

(4) In the fire model of the mine tunnel, the effect of various supports on the tunnel wall on the longitudinal ventilation speed is not considered, and the tunnel wall is set as a non-slip boundary condition.

III. THEORETICAL ANALYSIS

A. INITIAL ENVIRONMENTAL PARAMETERS

Altitude has significant effects on ambient temperature, atmospheric pressure, and oxygen concentration in the atmosphere. According to meteorological measurements, increasing every 100 m altitude, the ambient temperature will decrease by about 6.5 °, the atmospheric pressure will decrease by 5 mmHg (about 0.67 kPa), and the mass concentration of oxygen also decreases by about 6.6% [17].

TABLE 1. Initial environmental parameters at five altitudes.

Altitude z (m)	Temperature T_a (°C)	Pressure P_a (kPa)	Air density ρ_a (kg/m^3)	Oxygen mass fraction $W_{O_2,a}$ (kg/kg)
0	20	101.325	1.293	23.2%
1,000	20	89.874	1.069	21.5%
2,000	15	79.494	0.962	19.8%
3,000	9.5	69.624	0.888	18.1%
4,000	2	61.448	0.783	16.3%

Changes in these conditions will have a certain influence on the occurrence and development of fires, and the movement and spread of smoke. Tang *et al.* [12] pointed out that at lower pressures, reductions in air density and air entrainment will cause accelerated decay of smoke temperature along the tunnel. Therefore, the calculation of atmospheric pressure and air density is particularly important.

The formula for calculating the atmospheric pressure at altitude z is shown in (1) [18].

$$P_z = P_0 \exp\left(-\frac{Mgz}{R_0 T}\right) \tag{1}$$

where P_0 is the atmospheric pressure at sea level, M is the molar mass of air, g is the acceleration of gravity, z is the altitude, R_0 is the universal gas constant, and T is the absolute temperature of the atmosphere. The expression of acceleration of gravity with altitude is shown in (2).

$$d_g/d_z = -3.08769 \times 10^{-6}(1 - 0.0014437 \sin^2 \phi) \tag{2}$$

When calculating the gravitational acceleration at a location where the altitude is determined, a calculating reference location with the same latitude as the measurement place shall be selected, so that the gravitational acceleration at the measurement location can be calculated using (2). Therefore, in (2), d_g and d_z represent the increment of gravitational acceleration and the corresponding altitude difference between the measurement location and the calculating reference location, respectively, and ϕ represents the latitude value of the using location. The calculating reference location was selected as Xining City, Qinghai Province, China, with an altitude of 2,300 m, a gravitational acceleration of 9.7911m/s, and a latitude value of 38°.

Air density is calculated using (3).

$$\frac{\rho_z}{\rho_0} = \frac{P_z}{P_0} \tag{3}$$

where ρ_0 is the air density at sea level. After calculation, the initial environmental parameters of each altitude are show in Table 1.

It should be pointed out that the plateau area with an altitude of 4,000 meters and above is covered with snow all the year, and the temperature difference between day and night is large. Therefore, well tubs frozen, jar jammed by freezing, and water pipe fractured due to freezing are common hazards. However, the de-icing operation is difficult and unsafe. As a consequence, some heating measures are usually required to ensure operational efficiency and safety [19]. In addition, under anoxic conditions at high-altitude, it is necessary to increase the oxygen concentration in the working space to ensure the health and safety of workers. To solve the problem of anoxic oxygen in the production process of high-altitude mines, a lot of research has focused on the oxygen-intensifying ventilation technology and other oxygen-intensifying methods [20]. Therefore, there are more factors to consider at the altitude of 5,000 m, which is more complicated, so it is not considered in the current study.

B. ROOF TEMPERATURE

The roof temperature is one of the important parameters in mine fires, which has a large impact on roadway support, structure of strata, and roadway stability. The generated smoke will accumulate under the roadway roof due to the buoyancy, causing the temperature under the roof to rise rapidly. High temperatures for a long time will cause deformation failure of the roof strata and roadway support, which will cause potential safety hazards in the subsequent production process of the mine.

About the temperature characteristics under roof in tunnel fires, a large number of theoretical analyses and experimental studies have been carried out. Kurioka *et al.* [21] gave the empirical calculation formula for the maximum temperature under the ceiling in tunnel fires and the position of the maximum temperature. Based on Kurioka's research [21], Li *et al.* [22] considered the influence of ventilation velocity, and proposed a sectional calculation expression of the maximum ceiling temperature in tunnel fires. Lönnermark and Ingason [23] studied the ceiling temperature in tunnel fires through large-scale fire tests, and found that the temperature of the smoke was as high as 1,365 °. Hu *et al.* [24] investigated the temperature distribution under the tunnel ceiling in the one-dimensional expansion phase through a full-scale tunnel fire test combined with theoretical analysis. It was found that the dimensionless temperature rise under the tunnel ceiling was exponentially attenuated along the centerline of the tunnel. The longitudinal temperature distribution model of the ceiling in tunnel fire is derived.

$$\frac{\Delta T_x}{\Delta T_0} = \frac{T_x - T_a}{T_0 - T_a} = e^{-kx} \tag{4}$$

where, ΔT represents the temperature rise under the ceiling, T_x is the roof temperature in the point where the distance from the fire source is$x$ m (°C), T_0 is the roof temperature

directly above the ignition source (°C). T_a is the initial temperature (°C). Due to the change in environment parameters, the Kurioka and Li models are no longer applicable, but can provide theoretical support for revealing the effect of altitude on roof temperature in mine fires.

IV. NUMERICAL MODELING

A. MATHEMATICAL MODEL

With the rapid development of computer technology, computational fluid dynamics (CFD) technology has received increasing attention. Numerical simulation of turbulence has become one of the main means for predicting natural environments and engineering flows. Therefore, FDS was selected to run the physical model of fire. As a CAD code, FDS focuses on modeling thermal drive flow in terms of smoke and heat transfer. LES (large eddy simulation), one of the two numerical simulation methods provided by FDS, is used because it not only has a good effect in dealing with turbulence and buoyancy, but also has a parallel computing function using Message-Passing Interface (MPI) [25], which can greatly reduce calculation time and the demand for computer memory.

Turbulence simulation uses the Smagorinsky subgrid-scale (SGS) model widely used in LES. The turbulent viscosity defined in the FDS is obtained by balancing energy generation and dissipation. Assuming that the small scale is in equilibrium, the turbulence Smagorinsky model defined by FDS is shown in (5) [26].

$$\mu_{LEC} = \rho(C_s\Delta)^2[2\bar{S}_{ij} : \bar{S}_{ij} - \frac{2}{3}(\nabla \cdot \bar{u})^2]^{1/2} \tag{5}$$

where $\bar{S}_{ij}$ is defined by:

$$\bar{S}_{ij} = \frac{1}{2}\left(\frac{\partial \bar{u}_i}{\partial \bar{x}_j} + \frac{\partial \bar{u}_j}{\partial \bar{x}_i}\right) \tag{6}$$

The other diffusion parameters, the thermal conductivity and the material diffusivity, are related to the turbulent viscosity. As shown in (7).

$$k_{LEC} = \frac{\mu_{LEC} C_P}{Pr}, \quad (\rho D)_{LES} = \frac{\mu_{LES}}{S_C} \tag{7}$$

where, μ_{LES} is the turbulent viscosity, ρ is the fluid density, C_s is the Smagorinsky constant, Δ is the filter width in LES, $\bar{u}$ is the velocity vector, $\bar{S}_{ij}$ is the symmetric rate of strain tensor, k_{LES} is the turbulent thermal conductivity, D is the diffusivity coefficient, C_p is the specific heat capacity, Pr is the turbulent Prandtl number, S_C is the turbulent Schmidt number.

The combustion model is a mixed-fraction combustion model based on an infinitely fast reaction. The thermal radiation transfer effect is considered by solving the radiation equation of the gray gas. The finite difference method and the staggered grid system are used to discretize the filtered control equation. According to the relative size of the convection time scale and diffusion time scale in the calculation process, the time step is automatically adjusted to meet the Courant-Friedrichs-Lewy condition (CFL condition)

$$\delta_{t,\max}\left(\frac{|u_{ijk}|}{\delta x}, \frac{|v_{ijk}|}{\delta y}, \frac{|w_{ijk}|}{\delta z}\right) < 1 \tag{8}$$

In the formula, δ_x, δ_y, and δ_z are the sizes of the grid cells in the x, y, and z directions respectively, and the corresponding velocities are u_{ijk}, v_{ijk}, and w_{ijk}, δ_t is the time step.

The wall surface adopts non-slip boundary conditions, and the wall speed is 0. Both surfaces at the end of the tunnel are open to ambient conditions, and the left end (tunnel entrance) is designated as the airflow inlet, using velocity boundary condition. The interface connecting to the outside on the other side adopts an open boundary. Both the velocity gradient and the temperature gradient are 0. The environment in the tunnel is the same as the external environment. See Table 1 for details.

B. FIRE SCENARIO

Due to the complex underground environment of the mine, there have been many fire accidents caused by belt conveyor fires in recent years, and the losses are huge [27]. For example, on November 20, 2015, there was a major fire accident in Xinghua Coal Mine of Jixi Mining Company of Longmei Group, Heilongjiang Province, China, which resulted in 22 people's death. The direct cause of the accident was a belt fire. Therefore, the drift in the mine production system is selected as the fire site. The roadway is 100 m long and 4 m wide. Its cross-section is a three-center arch, and the distance between the roof and floor is 3.5 m. The roadway wall is made of concrete and its physical properties are specified by the FDS [28]. The wall thickness of the tunnel is 1 m. In the center of the roadway area, a square fire source with an area of 4 m^2 is placed at the bottom of the tunnel, and the reaction is n-heptane. The fire heat release rate involved in tests ranges from 10 MW to 150 MW [29].

Some research work has shown that FDS simulation with the extended computational domain will make the simulation results more accurate [30], [31] Therefore, the extended computational domain is added to the tunnel vent. Four rows of thermocouples with a diameter of 1 mm are arranged along the longitudinal centerline of the roadway, and a total of 80 thermocouples are used. In the horizontal direction, the interval between two thermocouples is 5 m, and in the vertical direction, every two thermocouples are spaced by 0.5 m. To measure the roof temperature in detail, the top row of thermocouples is 0.25 meters away from the roof.

It should be noted that mine tunnels are different from road tunnels or railway tunnels that are mainly naturally ventilated. Mine tunnels usually require mechanical ventilation to meet production requirements and ensure the safety conditions of the mine. As a consequence, the velocity supply surface is adopted at the boundary of the extended calculation domain at the entrance of the tunnel. According to the recommendation of China's safety regulations for metal and non-metal mine [32], the control ventilation velocity is 3 m/s. The numerical simulation scene is shown in Fig. 1.

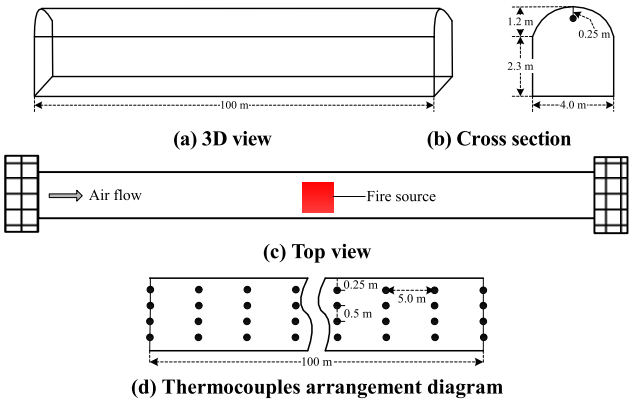

FIGURE 1. Schematic view of the tunnel model.

C. GRID SYSTEM SETUP

In the fire simulation calculation, the grid division is very important and unique [29]. If the grid is too small, the calculation results can be obtained more accurately, but the existing computer process will consume a lot of time and energy. On the contrary, if the grid is too large, the calculation accuracy will be affected, and the expected simulation effect will not be obtained. It has been proved that when the ratio of fire characteristic size to grid size $D^*/\delta x$ is between 4 and 16, the calculation results of FDS numerical simulation can accurately describe the changes of parameters in the model, and reliable results can be obtained when $\delta x = 0.1D^*$ [26]. The fire characteristic size D^* is determined using (9).

$$D^* = \left(\frac{Q}{\rho_a C_p T_a \sqrt{g}}\right)^{2/5} \tag{9}$$

Q is fire heat release rate (kW), ρ_a is the air density, C_p is the specific heat of air, take 1.014 $kJ/(kg \cdot K)$, T_a is the initial temperature (°C).

Due to the difference in atmospheric parameters in (9) under different altitude conditions, it is difficult to uniquely determine the value of D^* when the altitude changes. Therefore, the grid independence tests were carried out by selecting the two cases with altitudes of 0 m and 3,000 m. The test conditions are the initial environmental parameters corresponding to 0 m altitude and 3,000 m altitude given in Table 1. In order to improve the mesh density, the selected fire scale is 3 kW smaller than 10 MW (the smallest heat release rate in the current study), and the corresponding range of $D^*/16 \sim D^*/4$ is approximately 0.09∼0.46. Combined with the simulation scenario, five grid resolutions between 0.1 and 0.5 were selected as the testing scheme, and the fluid temperature measured at 1.2 m below the roof along the longitudinal centerline of the roadway was selected as the testing parameter. Table 2 gives the specific grid system and its corresponding test results. Fig. 2 presents the comparison of the temperatures of the five different grids at altitudes of 0 m and 3,000 m.

It can be found that the difference between the curves of test schemes 1∼3 (Test no. 1∼ 6) is very small, whether at 0 m altitude or 3000 m altitude. The third scheme (the grid accuracy of 0.25) is finally adopted to meet the good results in simulation precision and short calculation time.

TABLE 2. Sensitivity analysis of grid system.

Scheme no.	Test no.	Altitude (m)	Grid size	CPU time (h)
1	1	0	0.1	25.58
	2	3,000	0.1	25.63
2	3	0	0.2	10.92
	4	3,000	0.2	18.67
3	5	0	0.25	9.62
	6	3,000	0.25	17.78
4	7	0	0.4	5.34
	8	3,000	0.4	13.02
5	9	0	0.5	4.48
	10	3,000	0.5	11.77

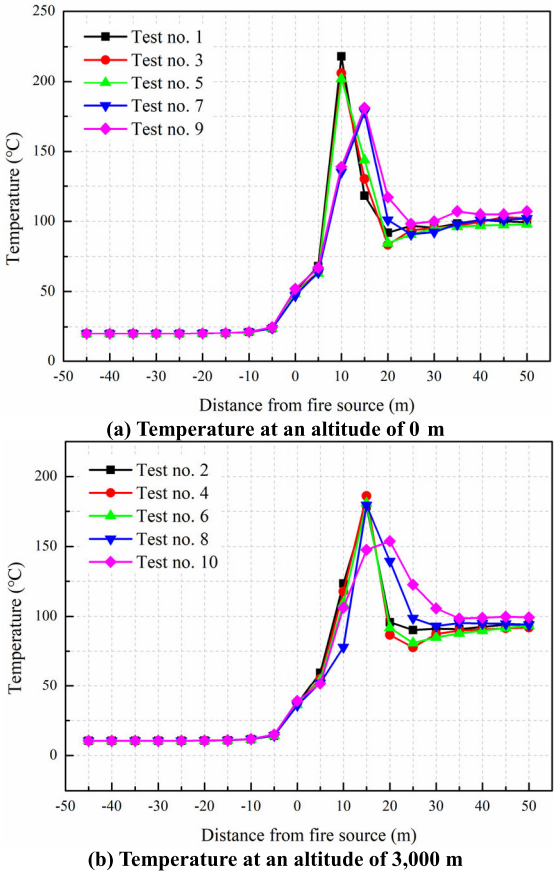

FIGURE 2. Prediction of temperature distribution in different grid systems.

V. RESULTS AND DISCUSSION

A. TIME DISTRIBUTION OF ROOF TEMPERATURE

In Fig. 3, taking the heat release rates of 10 MW and 150 MW as examples, the relationship between the roof temperature at 15m downstream of the fire source versus time with different altitudes is depicted.

It can be seen that when HRR is equal to 10 MW, the stable temperature in conventional-altitude tunnels (altitude $<$ 3000m) is lower than in high-altitude tunnels

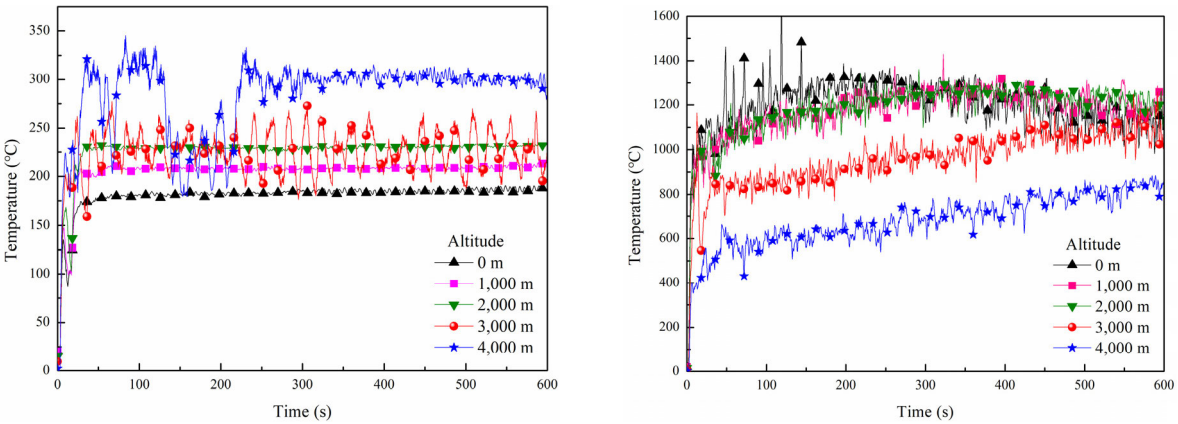

(a) HRR 10MW (b) HRR 150MW

FIGURE 3. Roof temperature versus time at different altitudes.

(altitude≥3,000 m). However, when HRR is equal to 150 MW, the phenomenon is just the opposite, the maximum temperature in the high-altitude tunnel is at a lower position. Remarkably, in the two graphs in Fig. 3, the temperature change curves in conventional-altitude tunnels are relatively smooth, and the fluctuation degree of the one in the high-altitude roadway is relatively large. Besides, the temperature difference between the tunnels at high altitudes is greater than at normal altitudes.

The main variables in tests are oxygen concentration, pressure, and temperature. Therefore, the reasons for the above phenomena will be analyzed from these three aspects. The first is oxygen concentration. Under small fire conditions, the size of the fire source is much smaller than the tunnel space. Therefore, the air supply in the tunnel environment is sufficient, and the combustion is intense and stable. At this time, the lack of oxygen in the air caused by the increase of altitude has no obvious effect on the fire, and the combustion in the simulated mine roadway is fuel-controlled combustion. Simultaneously, According to the conclusions of multiple studies [12]–[14], it can be seen that lower atmospheric pressure will reduce the air entrainment in the tunnel, while less entrained mass transportation will result in less heat loss. Eventually, the roof temperature in small fires at higher altitudes (indicating lower atmospheric pressure) is higher than in normal-altitude tunnels. When HRR continues to expand, the burning rate is dominated by ventilation conditions (oxygen). At this time, the combustion becomes unstable, and the intensity of combustion is closely related to the amount of oxygen supplied. However, as the rise of mine's altitude, the oxygen content in the tunnel decreases gradually, which results in secondary hypoxia during the combustion process. Therefore, when the scale of the fire is relatively large and the mine where the fire occurred is in a high-altitude area, the combustion is insufficient and unstable, and the roof temperature cannot reach the one in normal altitude. Different environmental temperatures also affect fire, it is well known that when other conditions are constant, the relationship between ambient temperature and fire intensity is positive correlation. So, the cold environment of high altitude can cool the fire to a certain extent and reduce the heat accumulation under the tunnel roof. On the whole, in mine fires at different altitudes, the roof temperature is affected by multiple factors simultaneously, which can be expressed by (10)

$$T_z = f(Q, W_{O_2,a}, P_a, T_a, C_p, g, H) \tag{10}$$

B. TEMPERATURE LONGITUDINAL DISTRIBUTION

Fig. 4 presents the gas temperature distribution beneath the roof (0.25 m away from the roof) along the longitudinal direction of the roadway with six HRR conditions. Mechanical ventilation inclines the flame downward to the wind side, so the maximum excess temperature on the longitudinal centerline is not directly above the fire source.

Fig. 4 shows that when HRR is relatively small (HRR<50 MW), the roof temperature increases as mine's altitude, which is consistent with the conclusions of multiple studies [12]–[15]. When the heat release rate increases to 50 MW, the roof temperature of the roadway increases at all altitudes. However, the temperature at the altitude of 4,000 m does not grow as fast as at other altitudes, resulting in the temperatures at the altitude of 2,000 m and 3,000 m higher than that at the altitude of 4,000 m. At this time, the roof temperatures at the other four altitudes still increase with the elevation except for the altitude of 4,000 m. As HRR continues to increase in Fig. 4 (e) and (f), the temperature along the longitudinal direction of the tunnel at high-altitude areas does not continue to rise, whereas the maximum temperature in the tunnels at 3,000 m and 4,000 m is stable at 800 ° and 1200 °, respectively, while the temperature in a normal altitude fire still increases with increase of HRR. It can be seen that the roof temperature decreases with increasing altitude at this time.

In summary, in mine fires at a normal altitude, when the altitude is kept constant, the roof temperature increases with the increase of heat release rate, and the change in altitude as little effect on the roof temperature. In mine fires at

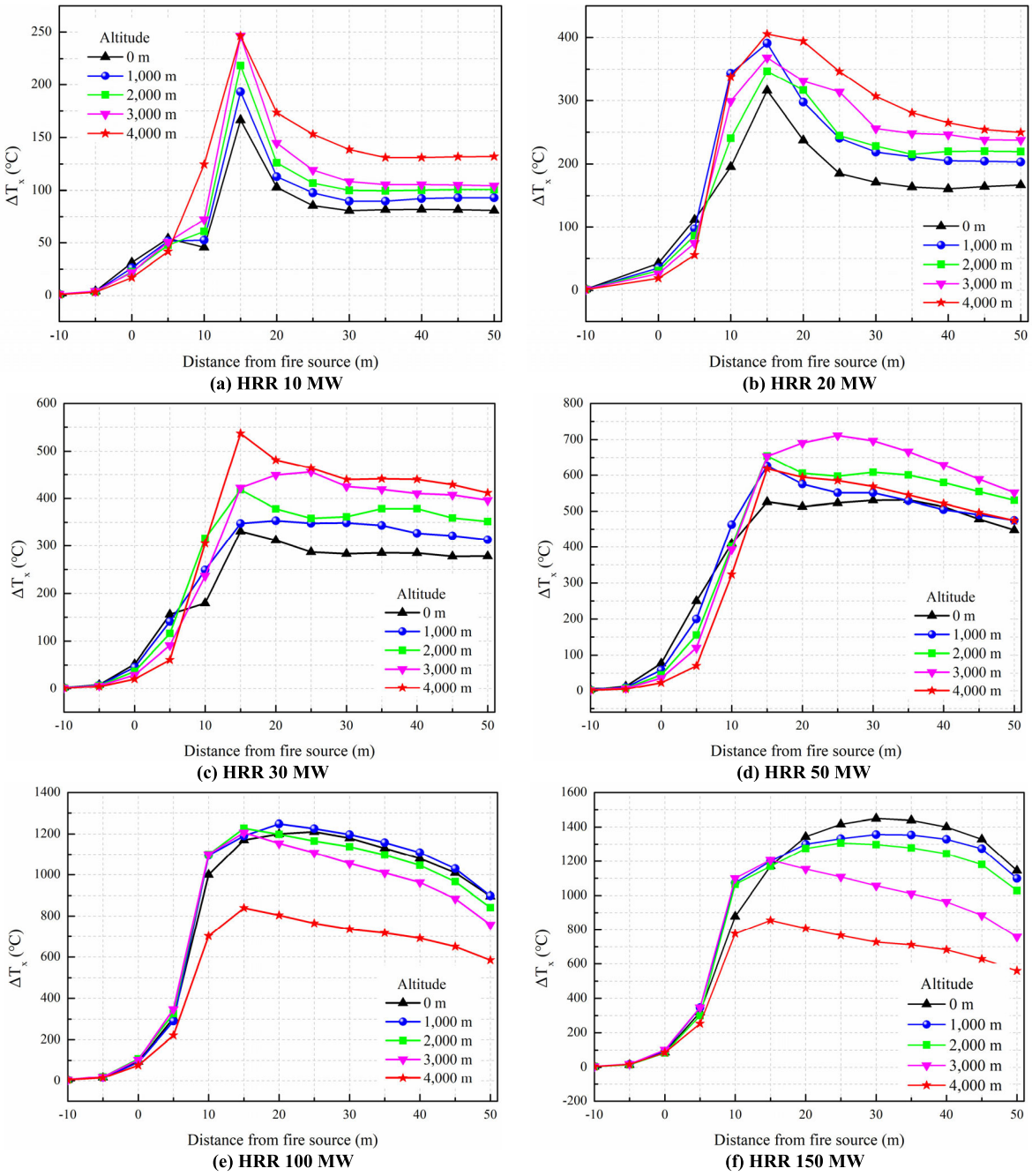

FIGURE 4. Temperature distribution beneath the roof at five altitudes with six fire sources.

a high altitude, changes in the environment have a great inhibitory effect on fire. When a fire occurs in a mine at the same altitude, the roof temperature increases with HRR, but it remains stable when HRR is 100 MW, and the higher the altitude, the lower the stable value of roof temperature. In addition, there are two modes of the influence of altitude on the roof temperature. When HRR is relatively small, the roof temperature increases with altitude, and when HRR is relatively large, the roof temperature decreases with increasing altitude. Therefore, when a fire occurs in a mine with a relatively high altitude, the damage of the roadway support is relatively small compared to the low-altitude area, and the roadway stability is relatively more guaranteed.

Combined with the analysis in Fig. 4, it can be seen that when HRR is relatively small, the influence of atmospheric pressure on the roof temperature is more important than the weight of oxygen concentration and the ambient temperature, so that the roof temperature in high-altitude tunnel is higher than that in low-altitude tunnel. This conclusion is also reflected in the experimental results of the aircraft cargo compartment [13] and Ji *et al.* [14], [35]. However, as HRR increases gradually, more oxygen is needed in the tunnel to support complete combustion of the fuel. Therefore, when HRR is increased gradually, the temperature in the high-altitude tunnel is little affected by the fire source, which is mainly controlled by ventilation (oxygen). When HRR is

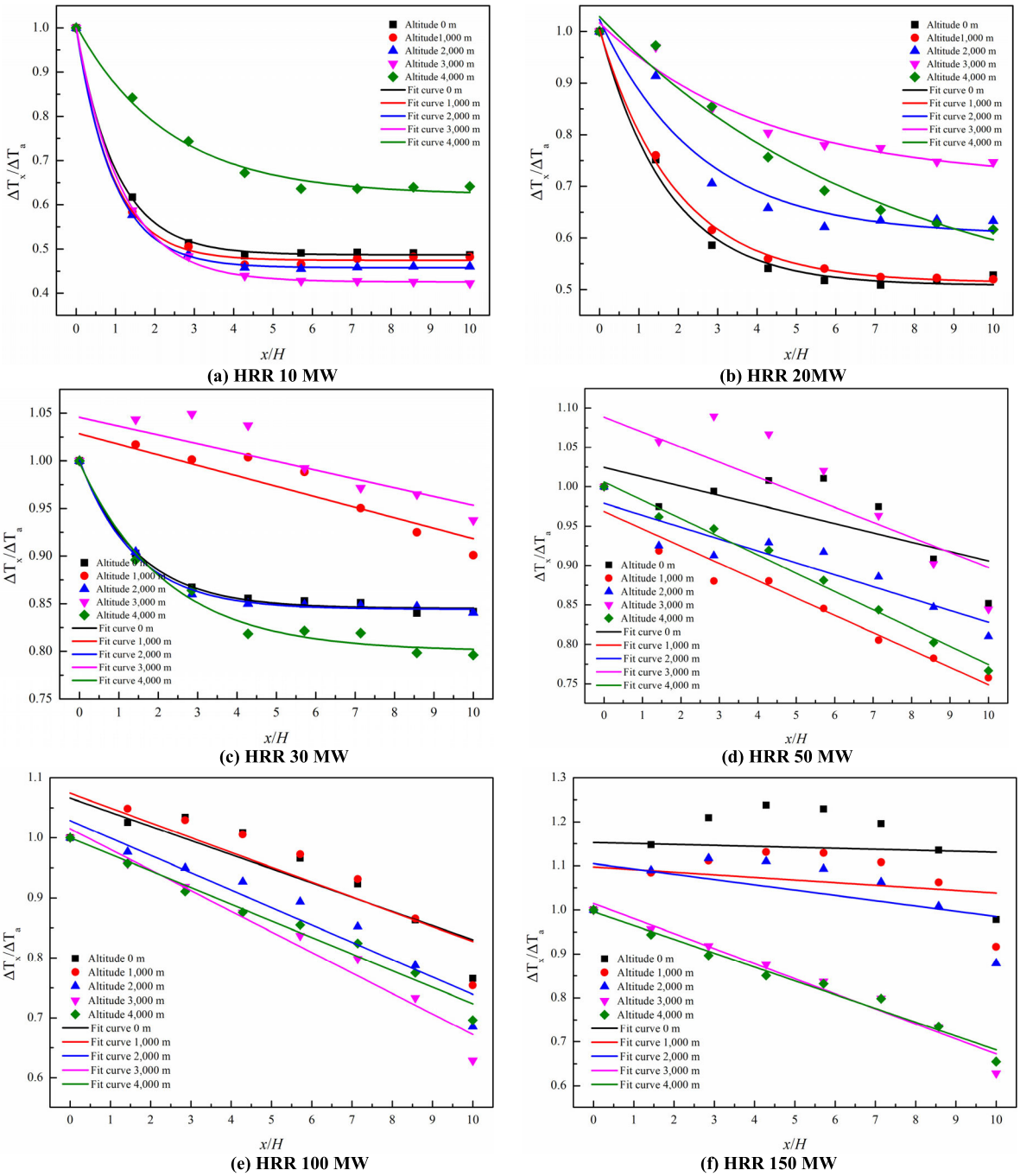

FIGURE 5. Distribution of dimensionless temperature rise.

increased from 100 MW to 150 MW, the roof temperature of the tunnel at the altitudes of 3,000 m and 4,000 m hardly increases, and the attenuation rate along the longitudinal direction of the tunnel is greater than that at a normal-altitude tunnel. The reason is that the attenuation effect of the oxygen supply is more dominant than that of air entrainment.

C. TEMPERATURE DECAY ANALYSIS

Because the peak temperature at the longitudinal center lineof the roadway does not show exactly above the fire source. In this paper, a virtual fire is used as a reference point, which represents the position of the maximum temperature of the center line when HRR is small, that is, 15 m away from the fire source in the downwind side of the fire source.

The curve between the dimensionless temperature rise along the longitudinal direction of the tunnel and the dimensionless distance based on the virtual fire source is plotted in Fig. 5. Where x is the horizontal distance from the measuring point to the virtual fire source, and H is the height of the roadway.

Fig. 5 shows that when HRR is less than 50MW, the dimensionless temperature rise exponentially decays against the dimensionless distance. However, when HRR is relatively large, the temperature no longer contents the

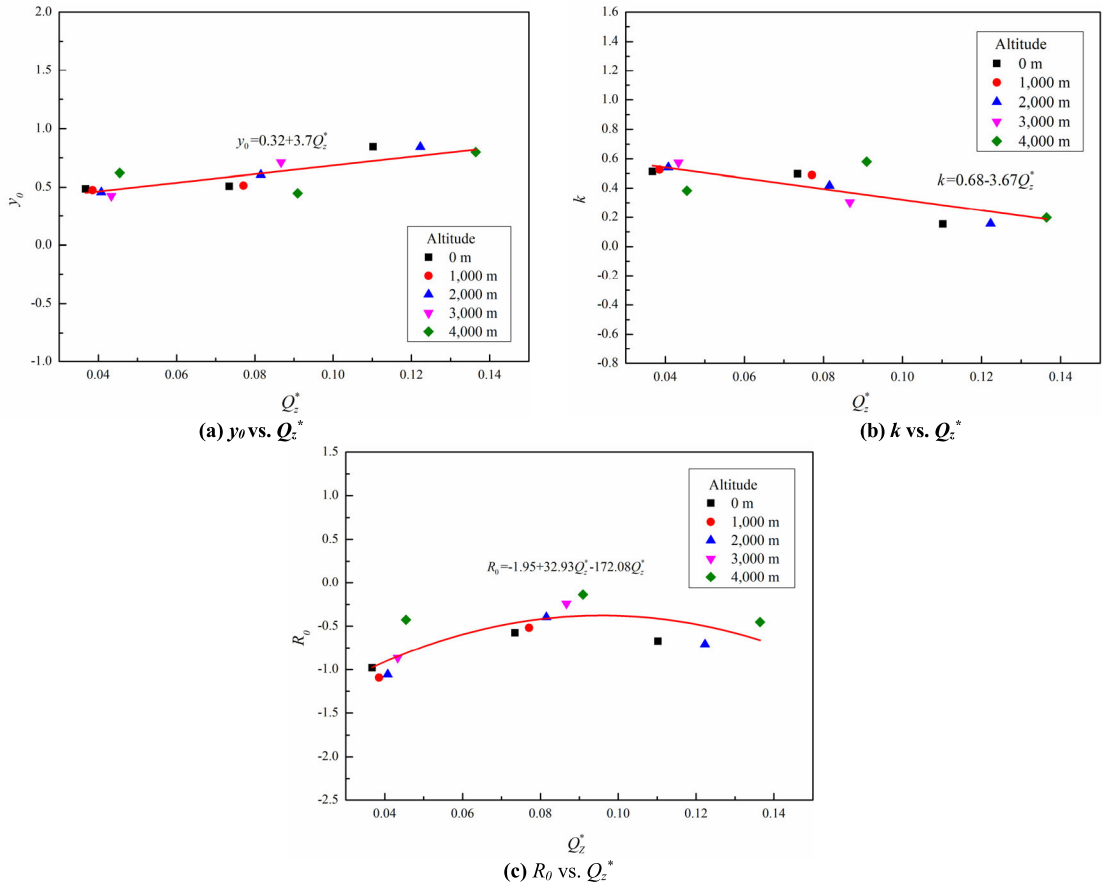

FIGURE 6. Variation of parameters, y_0, k and R_0, vs. dimensionless HRR.

exponential distribution. After repeated fitting attempts, it is found that the fitting of the corresponding data can be done well using a linear function.

According to the above analysis, in the process of continuously increasing HRR, the altitude of mine has two different influence modes on the roof temperature, and there are two functional relations between the dimensionless temperature rise and the dimensionless distance. Therefore, altitude is discussed in two cases. Assume dimensionless temperature rise as (11).

$$\frac{\Delta T_x}{\Delta T_a} = \begin{cases} y_0 + ke^{R_0(x/H)}, & HRR < 50MW \\ A + B(x/H), & HRR \geq 50MW \end{cases} \tag{11}$$

Formula (10) shows that in mine fires at different altitudes, the temperature beneath the roadway roof is not only related to the heat release rate of fuel, but also closely related to environmental factors such as oxygen concentration, pressure, and ambient temperature at various altitudes. Therefore, in (11), y_0, kR_0, A and B should be functions of altitude and fire heat release rate. A dimensionless heat release rate Q_z^* including pressure, oxygen mass fraction and initial ambient temperature can be defined as a measure of the temperature distribution of the roof when HRR and altitudechange. Based on dimensional analysis, (10) can be expressed as

$$D_z^* = \left(\frac{Q}{P_a C_p T_a H^{3/2} / W_{o_2,a} \sqrt{g}} \right) \tag{12}$$

Fig. 6 shows the points of the parameters y_0, k, and R_0 against dimensionless HRR. There is a linear relationship between y_0 and Q_z^*, k and Q_z^*, and the relationship between R_0 and Q_z^* is nonlinear. Therefore, when the heat release rate is relatively small, the fitting correlation between dimensionless temperature rise and Q_z^* is given by (13).

$$\frac{\Delta T_x}{\Delta T_a} = \begin{cases} 0.32 + 3.7Q_z^* \\ +(0.68 - 3.67Q_z^*)e^{R_0(x/H)} \\ R_0 = -1.95 \\ +32.93Q_z^* - 172.08Q_z^{*2}, \end{cases} \quad HRR < 50MW \tag{13}$$

Similarly, the relationship between A and Q_z^*, B and Q_z^* is depicted in Fig. 7. The expression of the temperature rise beneath the roof is (14).

$$\frac{\Delta T_x}{\Delta T_0} = (1.01 + 0.08Q_z^*) - 0.01(x/H), \quad Q \geq 50MW \tag{14}$$

When the reference point locates at the upright top position of virtual fire source, the final dimensionless temperature rise should be 1, indicating that y_0 plus k is equal to 1. Therefore, based on Fan's research [35], when considering the altitude of the mine where the fire occurred, the relationship between the dimensionless roof temperature rise and dimensionless heat release rate

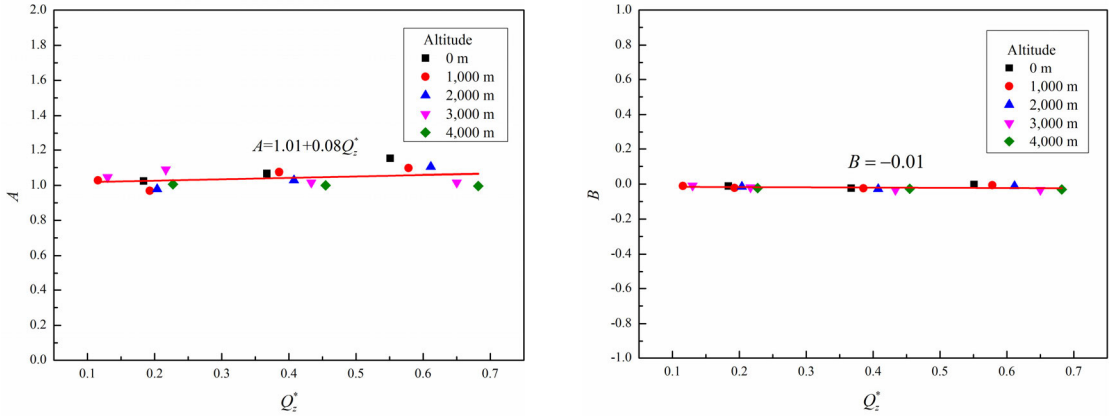

(a) A_z^* vs. Q (b) B_z^* vs. Q

FIGURE 7. Variation of parameters, *A* and *B*, vs. dimensionless HRR.

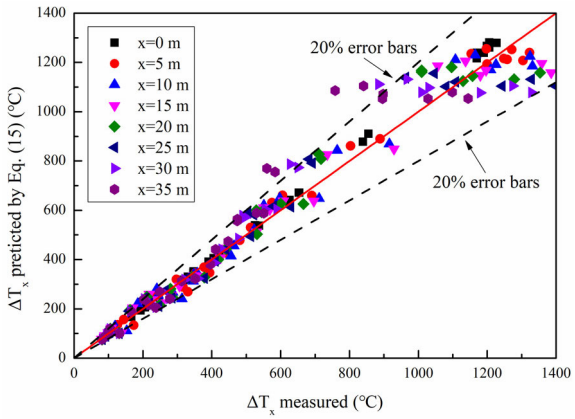

FIGURE 8. The comparison of longitudinal temperatures.

should be (15).

$$\frac{\Delta T_x}{\Delta T_a} = \begin{cases} 0.32+3.67Q_z^*+(0.68 \\ -3.67Q_z^*)e^{-1.95+32.93Q_z^*-172.08Q_z^{*2}(x/H)}, & HRR \\ & <50MW \\ (1.01+0.08Q_z^*)-0.01(x/H), & HRR \\ & \geq 50MW \end{cases} \quad (15)$$

The temperature calculated by (15) is compared with the temperature measured by thermocouples, and the result is shown in Fig. 8, which shows that the prediction effect is good.

VI. CONCLUSIONS

This study used the CFD code to simulate mine roadway fires at five different altitudes. It mainly focuses on the evolution of the temperature field and the smoke field beneath the roof of the mine roadway. The empirical correlation for predicting roof temperature distribution along the centerline of the tunnel was developed considering the effect of the mine's altitude, heat release rate, and using dimensionless analysis. The major findings include:

1) In mine fires at different altitudes, when the heat release rate is relatively small, the combustion belongs to fuel-controlled combustion, and the roof temperature increases with the altitude of the mine. When the heat release rate is relatively large, the roof temperature decreases gradually with mine's altitude, which is mainly due to the low oxygen environment in plateau areas.

2) In mine fires at conventional altitudes (altitude<3,000 m), changes in altitude have little effect on the roof temperature. The roof temperature is always positively correlated with the increasing heat release rate. In high-altitude mine fires, changes in altitude have an inhibitory effect on fire. At this time, the roof temperature also increases with the increase of heat release rate. However, it no longer continues to rise when the heat release rate increases to 100 MW. Instead, it remains stable, and the higher the altitude, the lower the stable value.

3) When a fire occurs in a mine at a relatively high altitude, the damage of the high-temperature smoke to the tunnel lining structure is smaller compared to the normal altitude, and the stability of the roadway is more guaranteed.

4) When there is a fire in a mine tunnel with longitudinal ventilation, the roof temperature along the centerline of the tunnel still has certain regularity. A virtual fire source is adopted at the downwind side of the fire source, which indicates the position of the peak temperature of the centerline when HRR is relatively small. In the process of continuously increasing the heat release rate, there are two types of correlations between the dimensionless roof temperature rise in the downstream region of the virtual fire source and the dimensionless distance based on the virtual fire source. The dimensionless downstream temperature rise decays exponentially against dimensionless distance in the case of a small fire, and it exhibits a linear correlation when HRR relatively large.

5) Through the combination of dimensional analysis and dimensionless analysis, a correlation formula for predicting the longitudinal distribution of roof temperature in mine fires at different altitudes was proposed. Through empirical research, it is found that the prediction of the empirical model is highly consistent with the measured data.

It should be pointed out that the ventilation velocity will change slightly in different stages of mine development.

However, due to the limitation of the length of the paper, to simplify the problem and emphasize the influence of mine's altitude, this study used the ventilation speed of 3 m/s recommended by China's safety regulations for metal and non-metal mines (GB 16423-2006) as the research condition, and proposed the basic idea of using numerical simulation method to study the influence of altitude on the roof temperature distribution in mine fires. Therefore, it is necessary to conduct further verification experiments on the simulation results, and conduct more experimental studies on the influence of altitude on smoke characteristics and temperature distribution at different ventilation speeds.

REFERENCES

[1] X. Lu, H. Zhu, D. Wang, C. Hu, H. Zhao, and Y. Huo, "Flow characteristic investigation of inhibition foam used for fire extinguishment in the underground goaf," *Process Saf. Environ. Protection*, vol. 116, pp. 159–168, May 2018.

[2] Z.-G. Yan, Y. Shen, H.-H. Zhu, X.-J. Li, and Y. Lu, "Experimental investigation of reinforced concrete and hybrid fibre reinforced concrete shield tunnel segments subjected to elevated temperature," *Fire Saf. J.*, vol. 71, pp. 86–99, Jan. 2015.

[3] A. Byström, X. Cheng, U. Wickström, and M. Veljkovic, "Full-scale experimental and numerical studies on compartment fire under low ambient temperature," *Building Environ.*, vol. 51, pp. 255–262, May 2012.

[4] L. H. Hu, F. Tang, M. A. Delichatsios, Q. Wang, K. H. Lu, and X. C. Zhang, "Global behaviors of enclosure fire and facade flame heights in normal and reduced atmospheric pressures at two altitudes," *Int. J. Heat Mass Transf.*, vol. 56, nos. 1–2, pp. 119–126, Jan. 2013.

[5] J. L. Deris, P. K. Wu, and D. G. Heskesta, "Radiation fire modeling," *Proc. Combustion Inst.*, vol. 28, no. 2, pp. 2751–2759, 2000.

[6] Z.-H. Li, Y. He, H. Zhang, and J. Wang, "Combustion characteristics of n-heptane and wood crib fires at different altitudes," *Proc. Combustion Inst.*, vol. 32, no. 2, pp. 2481–2488, 2009.

[7] Y. Zhang, J. Ji, J. Li, J. Sun, Q. Wang, and X. Huang, "Effects of altitude and sample width on the characteristics of horizontal flame spread over wood sheets," *Fire Saf. J.*, vol. 51, pp. 120–125, Jul. 2012.

[8] R. Tu, Y. Zeng, J. Fang, and Y. M. Zhang, "Influence of high altitude on the burning behaviour of typical combustibles and the related responses of smoke detectors in compartments," *Roy. Soc. Open Sci.*, vol. 5, no. 4, pp. 1–11. Apr. 2018.

[9] D. Bento, K. Thomson, and O. Gulder, "Soot formation and temperature field structure in laminar propane-air diffusion flames at elevated pressures," *Combustion Flame*, vol. 145, no. 4, pp. 765–778, Jun. 2006.

[10] R. Tu, Y. Zeng, J. Fang, and Y. Zhang, "The influence of low air pressure on horizontal flame spread over flexible polyurethane foam and correlative smoke productions," *Appl. Thermal Eng.*, vol. 94, pp. 133–140, Feb. 2016.

[11] H. I. Joo and Ö. L. Gülder, "Soot formation and temperature field structure in co-flow laminar methane-air diffusion flames at pressures from 10 to 60atm," *Proc. Combustion Inst.*, vol. 32, no. 1, pp. 769–775, 2009.

[12] F. Tang, L. H. Hu, L. Z. Yang, Z. W. Qiu, and X. C. Zhang, "Longitudinal distributions of CO concentration and temperature in buoyant tunnel fire smoke flow in a reduced pressure atmosphere with lower air entrainment at high altitude," *Int. J. Heat Mass Transf.*, vol. 75, pp. 130–134, Aug. 2014.

[13] J. Wang, S. Lu, Y. Guan, S. Lo, and H. Zhang, "Experiment investigation on the influence of low pressure on ceiling temperature profile in aircraft cargo compartment fires," *Appl. Thermal Eng.*, vol. 89, pp. 526–533, Oct. 2015.

[14] J. Ji, F. Guo, Z. Gao, J. Zhu, and J. Sun, "Numerical investigation on the effect of ambient pressure on smoke movement and temperature distribution in tunnel fires," *Appl. Thermal Eng.*, vol. 118, pp. 663–669, May 2017.

[15] Z.-G. Yan, Q.-H. Guo, and H.-H. Zhu, "Full-scale experiments on fire characteristics of road tunnel at high altitude," *Tunnelling Underground Space Technol.*, vol. 66, pp. 134–146, Jun. 2017.

[16] N. Zhang, Z. Tan, and M. Jin, "Research on the technology of disaster prevention and rescue in high-altitude super-long railway tunnel," *KSCE J. Civil Eng.*, vol. 19, no. 3, pp. 756–764, Mar. 2015.

[17] Z. H. Li, M. J. Yang, H. Zhang, and J. Wang, "Contrastive experiments and combustion characteristics of a square-pans fire under low pressure and low oxygen concentration in Tibet," *J. Univ. Sci. Technol. China*, vol. 39, no. 2, pp. 105–109, Feb. 2009.

[18] S. Xin, *Mine Ventilation in Plateau*. Beijing, China: Coal Industry Press, 2015.

[19] X. Tan, W. Chen, D. Yang, Y. Dai, G. Wu, J. Yang, H. Yu, H. Tian, and W. Zhao, "Study on the influence of airflow on the temperature of the surrounding rock in a cold region tunnel and its application to insulation layer design," *Appl. Thermal Eng.*, vol. 67, nos. 1–2, pp. 320–334, Jun. 2014.

[20] H. Zhong, N. L. Hu, G. Q. Li, and J. Hou, "On the oxygen-intensifying ventilation technology for plateau mine tunneling via the application of the software fluent," *J. Saf. Environ.*, vol. 17, no. 1, pp. 81–85. Feb. 2017.

[21] H. Kurioka, Y. Oka, H. Satoh, and O. Sugawa, "Fire properties in near field of square fire source with longitudinal ventilation in tunnels," *Fire Saf. J.*, vol. 38, no. 4, pp. 319–340, Jun. 2003.

[22] Y. Z. Li, B. Lei, and H. Ingason, "The maximum temperature of buoyancy-driven smoke flow beneath the ceiling in tunnel fires," *Fire Saf. J.*, vol. 46, no. 4, pp. 204–210, May 2011.

[23] A. Lönnermark and H. Ingason, "Gas temperatures in heavy goods vehicle fires in tunnels," *Fire Saf. J.*, vol. 40, no. 6, pp. 506–527, Sep. 2005.

[24] L. H. Hu, R. Huo, H. B. Wang, Y. Z. Li, and R. X. Yang, "Experimental studies on fire-induced buoyant smoke temperature distribution along tunnel ceiling," *Building Environ.*, vol. 42, no. 11, pp. 3905–3915, Nov. 2007.

[25] W. Gropp, E. Lusk, and A. Skjellum, "Using MPI: Portable parallel programming with the message-passing interface," *Sci. Program.*, vol. 5, no. 3, pp. 275–276, Jan. 1999.

[26] K. B. McGrattan, H. R. Baum, R. G. Rehm, A. P. Hamins, G. P. Forney, J. E. Floyd, and S. A. Hostikka, *Fire Dynamics Simulator, Technical Reference Guide*, 2th ed. Gaithersburg, MD, USA: National Institute of Standards and Technology, 2001.

[27] Q. J. Qi, H. Wang, and Z. W. Dong, "Numerical simulation of belt conveyor fire spreading law in coal mine," *China Saf. Sci. J.*, vol. 26, no. 10, pp. 36–41, Dec. 2016.

[28] S. Gannouni and R. B. Maad, "Numerical analysis of smoke dispersion against the wind in a tunnel fire," *J. Wind Eng. Ind. Aerodynamics*, vol. 158, pp. 61–68, Nov. 2016.

[29] H. Ingason, Y. Z. Li and A. LÖnnermark, *Tunnel Fire Dynamic*, 1st ed. New York, NY, USA: Springer, 2015, pp. 207–230.

[30] Y. He, C. Jamieson, A. Jeary, and J. Wang, "Effect of computation domain on simulation of small compartment fires," *Fire Saf. Sci.*, vol. 9, pp. 1365–1376, 2008.

[31] R. Ostilla-Mónico, R. Verzicco, and D. Lohse, "Effects of the computational domain size on direct numerical simulations of Taylor-couette turbulence with stationary outer cylinder," *Phys. Fluids*, vol. 27, no. 2, Feb. 2015, Art. no. 025110.

[32] *Safety Regulations for Metal and Nonmetal Mines*, document GB 16423-2006, General Administration of Quality Supervision, Inspection and Quarantine of the People's Republic of China, Beijing, China, 2006.

[33] X. Xu, H. Li, and Y. Lin, "Mesh–Order independence in CFD simulation," *IEEE Access*, vol. 7, pp. 119069–119081, 2019.

[34] J. Ji, F. Guo, Z. Gao, and J. Zhu, "Effects of ambient pressure on transport characteristics of thermal-driven smoke flow in a tunnel," *Int. J. Thermal Sci.*, vol. 125, pp. 210–217, Mar. 2018.

[35] C. G. Fan, J. Ji, Z. H. Gao, and J. H. Sun, "Experimental study on transverse smoke temperature distribution in road tunnel fires," *Tunnelling Underground Space Technol.*, vol. 37, pp. 89–95, Aug. 2013.

E WU is currently pursuing the M.S. degree with the School of Resources and Safety Engineering, Central South University, Hunan, China. Her research interests include safety science technology and mine disaster prevention.

RUI HUANG received the B.Eng. degree in engineering mechanics from the Nanjing University of Science and Technology, Nanjing, China, in 1998, and the Ph.D. degree in thermophysics from the University of Science and Technology of China, Hefei, China, in 2004. He is currently an Associate Professor with the School of Resources and Safety Engineering, Central South University. His research interests include safety science technology, safety management, and safety assessment.

LIN WU is currently pursuing the M.S. degree with the School of Resources and Safety Engineering, Central South University, Hunan, China. His research interests include safety science theory and safety informatics.

XUE SHEN is currently pursuing the M.S. degree with the School of Resources and Safety Engineering, Central South University, Hunan, China. His research interests include safety science technology and mine ventilation engineering.

ZEYOU LI is currently pursuing the M.S. degree with the School of Resources and Safety Engineering, Central South University, Hunan, China. His research interests include safety science technology and mine disaster prevention.